Materials Science Forum
ISSN: 1662-9752, Vol. 885, pp 74-79
doi:10.4028/www.scientific.net/MSF.885.74

Submitted: 2016-02-11
Revised: 2016-09-15
Accepted: 2016-09-15
Online: 2017-02-10

Investigation of Lattice Defects in a Plastically Deformed High-Entropy Alloy

Anita Heczel[1,a *], Yi Huang[2,b], Terence G. Langdon[2,c], Jenő Gubicza[1,d]

[1]Department of Materials Physics, Eötvös Loránd University, Budapest, Hungary

[2]Materials Research Group, Faculty of Engineering and the Environment, University of Southampton, Southampton, UK

[a]heczel.anita@gmail.com, [b]Y.Huang@soton.ac.uk, [c]langdon@usc.edu, [d]jeno.gubicza@ttk.elte.hu

Keywords: High-Entropy Alloy, X-ray Diffraction, Dislocations, Plastic Deformation, Phase Transformation

Abstract. The lattice defect structure developed during plastic deformation in a High-Entropy Alloy (HEA) with the composition of $Ti_{35}Zr_{27.5}Hf_{27.5}Nb_5Ta_5$ was investigated. The crystallite size as well as the density of dislocations in a disk processed by High-Pressure Torsion (HPT) were determined by X-ray line profile analysis (XLPA). Additional transmission electron microscopy (TEM) investigations were carried out to monitor the grain size evolution during deformation. It was found that the dislocation density in the HPT-processed sample was very high compared to conventional materials. In addition, in $Ti_{35}Zr_{27.5}Hf_{27.5}Nb_5Ta_5$ HEA the initial body-centered cubic structure transformed into a martensitic phase during HPT. The hardness of this HEA was investigated along the HPT-processed disk radius and correlated to the microstructure.

Introduction

High entropy alloys (HEAs) represent a new class of materials. These alloys are currently the focus of materials science and engineering because they have excellent mechanical performance [1-4]. HEAs are disordered solid solutions, containing five or more principal elements in equal or near-equal atomic ratios, in which all the atomic concentrations are between 5% and 35% [1]. The disordered crystal lattice of HEA materials yields strong resistance to dislocation motion, resulting in a high strength even if the grain size is large [5]. A study of the plastic properties in HEAs is of great importance from the point of view of their practical applications. In a recently published paper, the room-temperature compressive behavior of an equimolar TiZrHfNbTa HEA was studied by transmission electron microscopy (TEM) [6]. The dislocation patterns and the activated slip systems were analyzed in detail in order to comprehend the dislocation-controlled mechanisms of plastic deformation at room temperature.

For a study of the plastic behavior of HEAs at high strains, severe plastic deformation (SPD) techniques must be applied. High pressure torsion (HPT) is one of the most effective SPD techniques in achieving high strength in structural materials [7-9]. It has been shown recently [10] that HPT-processing yielded an additional improvement in hardness of a CoCrFeNiMn HEA due to grain refinement into the nanocrystalline regime. Annealing after HPT-processing for a $Al_{0.3}$CoCrFeNi HEA yielded additional hardening [11]. A study of the evolution of defect structure (e.g. the type and density of dislocations) during SPD-processing of HEAs is fundamental in understanding their deformation mechanisms.

The correlation between dislocation density and mechanical behavior for a refractory HEA with equiatomic composition ($Ti_{20}Zr_{20}Hf_{20}Nb_{20}Ta_{20}$) was studied in recently published reports [5,12]. The dislocation density and the edge/screw character of dislocations during quasistatic compression tests were studied by X-ray line profile analysis (XLPA). To determine these parameters of the microstructure, the elastic anisotropy factor must be known and this is not available in the literature. Therefore, the elastic anisotropy factor for XLPA procedure was determined using a depth-sensing indentation technique [13]. This anisotropy factor was used for an estimation of the parameter q which describes the edge/screw character of dislocations. The analysis gave 2.65 ± 0.05 and 1.10 ±

0.50 for the theoretical values of parameter q in the case of pure screw and edge dislocations, respectively [5]. A comparison of the theoretically calculated and the experimentally obtained q values suggested that, with increasing strain during compression, the dislocation character became more screw. XLPA showed that the crystallite size decreased while the dislocation density increased with increasing strain during compression, and their values reached ~39 nm and ~15 × 10^{14} m^{-2}, respectively, at a plastic strain of ~20% [5]. A much larger average dislocation density was achieved under dynamic loading conditions. For instance, at a strain rate of 4700 s^{-1} the dislocation density in $Ti_{20}Zr_{20}Hf_{20}Nb_{20}Ta_{20}$ HEA reached 47 × 10^{14} m^{-2} which is larger than the value obtained in quasi-statically compressed specimens at similar imposed strains (15 × 10^{14} m^{-2}) [12]. For both quasi-statically and dynamically loaded specimens, the strength was successfully correlated to the dislocation density using the Taylor equation [5,12].

In the present work, the plasticity induced evolution of the density of dislocations is studied in a $Ti_{35}Zr_{27.5}Hf_{27.5}Nb_5Ta_5$ HEA with body-centered cubic (bcc) structure. The Ti-rich $Ti_{35}Zr_{27.5}Hf_{27.5}Nb_5Ta_5$ HEA was processed by HPT for 1 turn. The dislocation density was determined by XLPA as a function of the distance from the center of the HPT-processed disk. X-ray diffraction also reveals that, in addition to the refinement of the microstructure and the increase of the dislocation density, a martensitic phase transition occurred during HPT.

Experimental procedures

A Ti-rich HEA with a composition of $Ti_{35}Zr_{27.5}Hf_{27.5}Nb_5Ta_5$ was prepared by arc melting under argon atmosphere and its microstructure is described elsewhere [4]. The as-cast material was thermo-mechanically treated in order to achieve a recrystallized microstructure using two steps of cold-rolling and annealing at 1200 °C for 24 h. A disk with a diameter of 9.85 mm and a thickness of ~0.85 mm was fabricated from the recrystallized alloy and processed by HPT for 1 turn. The HPT facility operated under quasi-constrained conditions with an applied pressure of 6.0 GPa and a rate of 1 rpm at room temperature [14].

The initial microstructure of the Ti-rich material was studied by optical microscopy. The size and morphology of grains in the HPT-processed sample were investigated by TEM using a Tecnai F20 FEG microscope operating at 200 kV. The phase composition and the average lattice parameters for the initial and HPT-processed samples were investigated by X-ray diffraction (XRD) using a Philips Xpert Θ–2Θ powder diffractometer with CuKα radiation (wavelength: λ = 0.15418 nm). The lattice parameter was determined by extrapolating the lattice parameters obtained from the different reflections to the diffraction angle of 2Θ = 180° using the Nelson–Riley method [15]. The microstructure of the HPT-processed sample was examined by XLPA. In the case of the HPT sample, the analysis was carried out at the center, half-radius and periphery of the disk. The X-ray line profiles were measured by a high-resolution rotating anode diffractometer (type: RA-MultiMax9, manufacturer: Rigaku) using CuKα_1 radiation (wavelength, λ = 0.15406 nm). The Debye-Scherrer diffraction rings were detected on two-dimensional imaging plates having a linear spatial resolution of 50 μm. The diffraction patterns were evaluated by the Convolutional Multiple Whole Profile (CMWP) analysis [16]. In this procedure, the diffraction pattern is fitted by the sum of a background spline and the convolution of the instrumental pattern and the theoretical line profiles related to crystallite size and dislocations. The area-weighted mean crystallite size ($\langle x \rangle_{area}$) and the dislocation density (ρ) were determined by the CMWP fitting evaluation procedure of the diffraction patterns. The value of $\langle x \rangle_{area}$ is calculated as $\langle x \rangle_{area} = m \cdot \exp(2.5\sigma^2)$, where m is the median and σ^2 is the log-normal variance of the crystallite size distribution [16]. The microhardness along the radius of the HPT disk was measured using a Zwick Roell ZHμ Vickers indenter with an applied load of 500 g and a dwell time of 10 s. The spacing between the neighboring indents was 0.5 mm.

Results and discussion

Figure 1a shows the X-ray diffraction pattern obtained for the initial undeformed Ti-rich HEA sample. The initial material has a bcc structure with a lattice parameter of ~0.345 nm. After 1 turn of HPT all of the material was transformed into a martensitic structure, as revealed by the XRD pattern recorded at the half-radius of the HPT-processed disk (see Fig. 1b). The new phase was indexed as an orthorombic structure with lattice parameters of a = 0.314 nm, b = 0.531 nm and c = 0.490 nm. It should be noted that a similar XRD diffractogram was obtained for the as-cast state (before recrystallization) for which the structure was also determined as orthorhombic with an orthorhombicity of 98% [4].

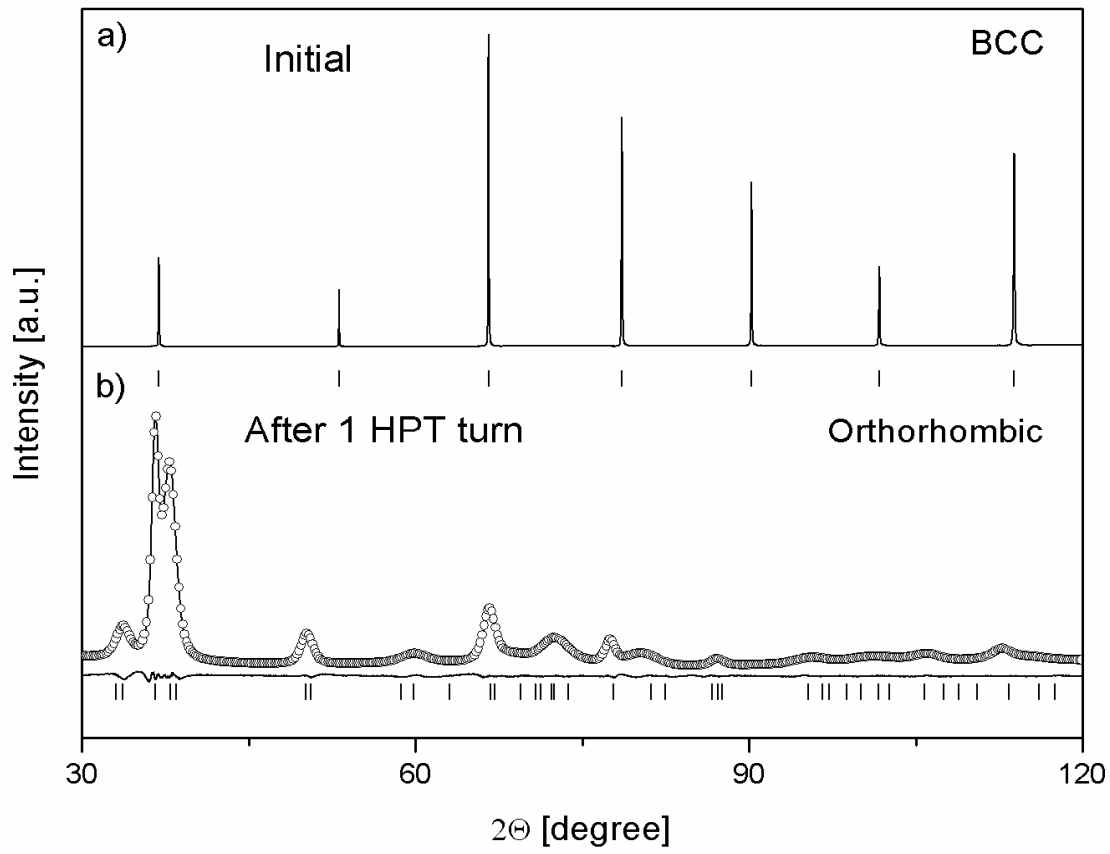

Fig. 1. XRD patterns for (a) the initial $Ti_{35}Zr_{27.5}Hf_{27.5}Nb_5Ta_5$ HEA sample and (b) the half-radius of the disk processed by 1 turn of HPT. The peak positions are indicated by small vertical lines. In (b) the experimental diffractogram and the theoretical pattern fitted by the CMWP method are represented by open circles and a solid line, respectively. The difference between the experimental and theoretical patterns is also shown at the bottom of the figure.

The microstructure of the orthorombic phase after 1 turn of HPT was examined by XLPA. The XLPA evaluation revealed that there is no significant difference between the crystallite size values observed at the center, half-radius and periphery of the disk. The average crystallite size was in the range 11-16 nm. At the same time, the dislocation density increased with increasing the distance from the disk center. Its values were ~4×10^{15} m^{-2} and ~10×10^{15} m^{-2} at the disk center and periphery, respectively (see Table 1). The very high dislocation density even after one turn of HPT can be explained by a reduced annihilation rate of dislocations during deformation which may be caused by the high stress required for dislocation motion in highly-alloyed HEA materials [5].

Table 1. The parameters of the microstructure obtained by XLPA. $\langle x \rangle_{area}$ is the area-weighted mean crystallite size and ρ is the dislocation density.

Location in the HPT disk	$\langle x \rangle_{area}$ [nm]	ρ [10^{15} m^{-2}]
Center	13 ± 2	4 ± 1
Half-radius	11 ± 2	8 ± 1
Periphery	16 ± 2	10 ± 1

The optical micrograph in Fig. 2a shows the microstructure of the initial sample before HPT deformation. The average grain size was determined as ~800 μm. The microstructure obtained by TEM at the half-radius of the HPT disk is shown in Fig. 2b. In the HPT-processed sample many grains are elongated with a broad size distribution. The average thickness and length of the grains are ~200 and ~1000 nm, respectively. It is noted that the crystallite size is much smaller than the grain size obtained by TEM. This difference can be explained by the fact that XLPA measures the size of sub-grains or dislocation cells rather than the true grain size.

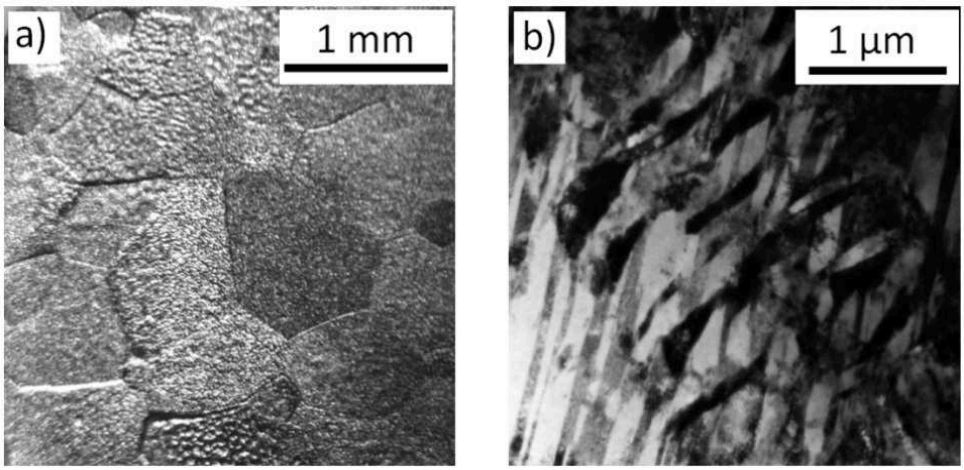

Fig. 2. Microstructure evolution in $Ti_{35}Zr_{27.5}Hf_{27.5}Nb_5Ta_5$ HEA during 1 turn of HPT: (a) Optical micrograph of the initial recrystallized sample, (b) TEM image showing the microstructure at the half-radius of the disk after 1 turn of HPT.

The onset of a phase transformation occurring during plastic deformation in the present HEA material was investigated by deforming the initial sample by uniaxial compression. After compression up to a strain of 5% the material was partially transformed from bcc to an orthorhombic structure. The EBSD image in Fig. 3a shows that the orthorhombic phase formed as lamellae in the bcc grains. This lamellar grain morphology was inherited in the elongated form of the grains in the HPT-processed sample (see Fig. 2b) where all of the material has already transformed into an orthorhombic structure. Compositional differences between the bcc and orthorhombic phases were not observed by energy dispersive spectroscopy, which confirms that the phase transformation is martensitic without diffusion. After 10% of compression (see Fig. 3b) only a minor fraction of the material remained as a bcc structure which indicates that the phase transformation during HPT most probably occurred already at the beginning of deformation.

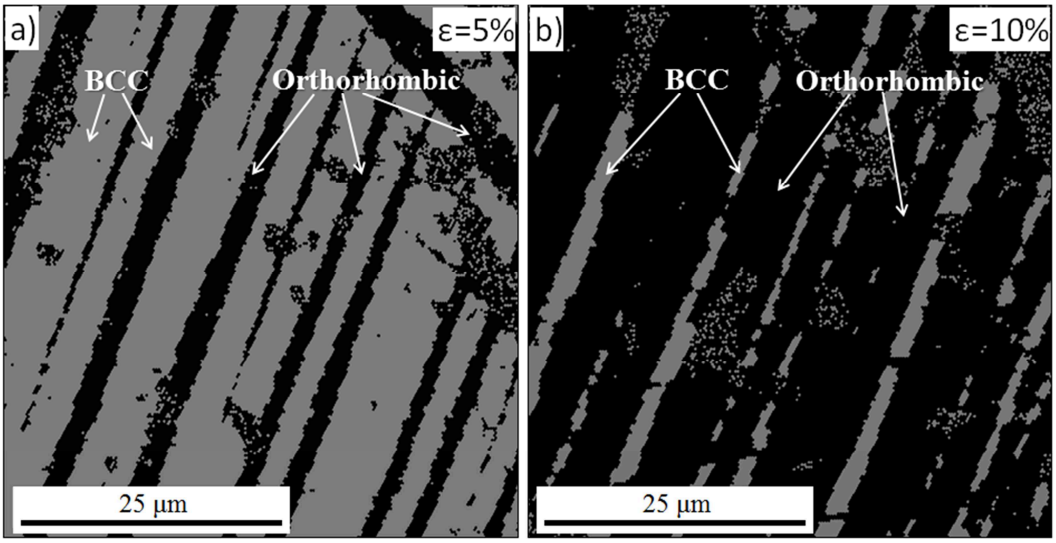

Fig. 3. EBSD images showing the bcc and orthorombic phases after compression for the strain of 5% (a) and 10% (b) (the light and the dark regions represent the lamellae of bcc and orthorombic phases, respectively).

The hardness in the center of the HPT-processed disk is ~3500 MPa which increases slightly towards the disk edge. At the periphery of the sample the hardness is ~3900 MPa. The difference between the hardness values measured at the center and the periphery can be attributed to the variation of the dislocation density along the disk radius (see Table 1), since both the phase composition and the grain size remain practically unchanged with increasing distance from the center. It is worth noting that the dislocation density is very high and the microstructure is ultrafine-grained even in the center of the disk processed by 1 turn of HPT where the nominal plastic strain is very small. This observation suggests an early saturation of the microstructure during HPT processing of this Ti-rich HEA material.

Summary

A Ti-rich HEA with a composition of $Ti_{35}Zr_{27.5}Hf_{27.5}Nb_5Ta_5$ was processed by 1 turn of HPT. The evolutions of the phase composition, microstructure and hardness were studied. The following conclusions were obtained:

1. Due to HPT-processing the initial grain size (~800 μm) was refined to ~200-1000 nm irrespective of the location along the disk radius. In this Ti-rich HEA material, besides the refinement of the microstructure, a phase transition also occurred during HPT. The initial bcc phase was transformed into a martensitic structure throughout the disk. The martensitic phase was identified as an orthorombic structure. The dislocation density in the martensitic phase increased to a very large value of $\sim 10^{16}$ m^{-2} at the periphery of the disk processed by 1 turn of HPT.
2. A very high hardness with values between 3500-3900 MPa was measured on the HPT-processed sample which changed only slightly along the disk radius in accordance with the microstructural observations. These results indicate a very early saturation of the microstructure and the hardness with increasing strain imposed in HPT-processing.

Acknowledgements

This work was supported by the Hungarian Scientific Research Fund, OTKA, Grant No. K-109021. The authors are grateful to Guy Dirras, Jean-Philippe Couzinié, Lola Lilensten, Julie Bourgon and Loic Perrière for the sample preparation and the TEM investigation. YH and TGL were supported by the European Research Council under ERC Grant Agreement No. 267464-SPDMETALS.

References

[1] J.W. Yeh, S.K. Chen, S.J. Lin, J.Y. Gan, T.S. Chin, T.T. Shun, C.H. Tsau, S.Y. Chang, Nanostructured high-entropy alloys with multiple principal elements: novel alloy design concepts and outcomes, Adv. Eng. Mater. 6 (2004) 299-303.

[2] D.B. Miracle, J.D. Miller, O.N. Senkov, C. Woodward, M.D. Uchic, J. Tiles, Exploration and development of high entropy alloys for structural applications, Entropy 16 (2014) 494-525.

[3] Z. Zou, H. Ma, R. Spolenak, Ultrastrong ductile and stable high-entropy alloys at small scales, Nature Comm. 6 (2015) 1-6.

[4] L. Lilensten, J.P. Couzinié, L. Perrière, J. Bourgon, N. Emery, I. Guillot, New structure in refractory high-entropy alloys, Mater. Lett. 132 (2014) 123-125.

[5] G. Dirras, J. Gubicza, A. Heczel, L. Lilensten, J.-P. Couzinié, L. Perrière, Y. Guillot, A. Hocini, Microstructural investigation of plastically deformed Ti20Zr20Hf20Nb20Ta20 high entropy alloy by X-ray diffraction and transmission electron microscopy, Mater. Char. 108 (2015) 1-7.

[6] J.P. Couzinié, L. Lilensten, Y. Champion, G. Dirras, L. Perrière, I. Guillot, On the room temperature deformation mechanisms of a TiZrHfNbTa refractory high-entropy alloy, Mater. Sci. Eng. A 645 (2015) 255-263.

[7] T.G. Langdon, Twenty-five years of ultrafine-grained materials: Achieving exceptional properties through grain refinement, Acta Mater. 61 (2013) 7035-7059.

[8] R.Z. Valiev, A.P. Zhilyaev, T.G. Langdon, Bulk Nanostructured Materials, Fundamentals and Applications, John Wiley & Sons, Inc., Hoboken, New Jersey, 2014.

[9] A.P. Zhilyaev, T.G. Langdon, Using high-pressure torsion for metal processing: Fundamentals and applications, Prog. Mater. Sci. 53 (2008) 893-979.

[10] D.H. Lee, I.C. Choi, M.Y. Seok, J. He, Z. Lu, J.Y. Suh, M. Kawasaki, T.G. Langdon, J.I. Jang, Nanomechanical behavior and structural stability of a nanocrystalline CoCrFeNiMn high-entropy alloy processed by high-pressure torsion, J. Mater. Res. 30 (2015) 2804-2815.

[11] Q.H. Tang, Y. Huang, Y.Y. Huang, X.Z. Liao, T.G. Langdon, P.Q. Dai, Hardening of an Al0.3CoCrFeNi high entropy alloy via high-pressure torsion and thermal annealing, Mater. Lett. 151 (2015) 126–129.

[12] G. Dirras, H. Couque, L. Lilensten, A. Heczel, D. Tingaud, J.-P. Couzinié, L. Perrière, J. Gubicza, I. Guillot, Mechanical behavior and microstructure of Ti20Hf20Zr20Ta20Nb20 high-entropy alloy loaded under quasi-static and dynamic compression conditions, Mater. Char. 111 (2016) 106–113

[13] J.J. Vlassak, W.D. Nix, Measuring the elastic properties of anisotropic materials by means of indentation experiments, J. Mech. Phys. Solids 42 (1994) 1223-1245.

[14] R.B. Figueiredo, P.H.R. Pereira, M.T.P. Aguilar, P.R. Cetlin, T.G. Langdon, Using finite element modelling to examine the flow processes in quasi-constrained high-pressure torsion, Acta Mater. 60 (2012) 3190-3198.

[15] J. Nelson, D. Riley, An experimental investigation of extrapolation methods in the derivation of accurate until-cell dimensions of crystals Proc. Phys. Soc. Lond. 57 (1945) 160-177.

[16] G. Ribárik, J. Gubicza, T. Ungár, Correlation between strength and microstructure of ball-milled Al–Mg alloys determined by X-ray diffraction, Mater. Sci. Eng. A 387-389 (2004) 343-347.